Published in the USA
Biogeosystem Technique
Issued since 2014.
E-ISSN: 2413-7316
2025. 12(1): 48-60

DOI: 10.13187/bgt.2025.1.48
https://bgt.cherkasgu.press

Assessment of Soil Erosion and Mitigation Strategies in Nghe An Province, Vietnam under Tropical Monsoon Conditions

Ha Thi Nguyen Thuy [a, *], Tamara S. Astarkhanova [b], Alla A. Okolelova [c], Van Tran Quang [d]

[a] School of Agriculture and Resources, Vinh University, Nghe An, Vietnam
[b] Agrarian Technological Institute, Patrice Lumumba Peoples' Friendship University of Russia, Moscow, Russian Federation
[c] Volgograd State Technical University, Russian Federation
[d] Tan Trao University, Tuyen Quang, Vietnam

Paper Review Summary:
Received: 2025, February 28
Received in revised form: 2025, April 15
Acceptance: 2025, April 26

Abstract

This study on soil erosion in Thanh Chuong, Nghe An Province (Vietnam) utilized GIS, remote sensing, and the RUSLE model to assess and quantify erosion dynamics. It was found that soil erosion is primarily influenced by the intensity and duration of monsoon rainfall, while the erosion resistance of landscapes is determined by factors such as slope, vegetation cover, and precipitation. High erosion rates were observed in areas where land use was mismatched with local agro-climatic conditions, leading to significant soil loss. The agroecological assessment revealed that 18 % of the study area experiences high to very high erosion, with an average annual soil loss of 25 T/ha. Erosion data were categorized based on three agricultural systems: tea and citrus cultivation along contour lines, annual crops on sloping lands, and perennial crops such as acacia and cassava. Using remote sensing and GIS, erosion was classified into five levels, ranging from very low to very high, while LS-Factor assessments from Landsat 8 images were divided into eight classes. To combat erosion, the study proposes several mitigation measures, including evaluating vegetation cover for anti-erosion efficiency, constructing trenches and embankments, creating terraced slopes, and optimizing agricultural and forestry practices through the SALT models for heavily eroded lands.

Keywords: soil erosion, RUSLE model, SALT model.

1. Introduction

Soil erosion is a critical exogenous geological process characterized by the detachment, transport, and deposition of soil particles due to hydrodynamic forces from surface water (water erosion) or aeolian activity (wind erosion or deflation). Its intensity is governed by soil properties, granulometric composition, vegetation cover, regional geomorphology, and land management practices (Aksoy, Kavvas, 2005). Globally, approximately 70 % of nations experience soil erosion and desertification, affecting 30 % of the continental landmass (Tian et al., 2008). In Vietnam,

[*] Corresponding author
E-mail addresses: hantt_dly@vinhuni.edu.vn (H. Thi Nguyen Thuy)

approximately 40 % of the national territory is subject to erosion, threatening agricultural productivity and socio-economic stability, particularly in East Asian nations such as Nepal, Malaysia, and Vietnam. Wischmeier and Smith identified topography, climate, soil characteristics, and anthropogenic influences as primary drivers of erosion (Le et al., 2022; Wischmeier, Smith, 1978).

Soil erosion leads to landscape degradation, water quality deterioration, and adverse socio-economic consequences (Golkarian et al., 2023). Unsustainable agricultural practices, deforestation, and climate change intensify its impacts (Adornado et al., 2009). In Vietnam's mountainous regions, agricultural activities on steep slopes (>25°) accelerate erosion, resulting in rapid soil depletion and a reduction in arable land (Committee T.C.D.P.s, 2021). Additionally, deforestation for artificial plantations, particularly acacia, exacerbates soil erosion. Research indicates that young acacia plantations are highly vulnerable due to insufficient vegetation cover, whereas mature plantations improve soil stability through extensive root networks. To promote sustainable development, the identification of erosion-prone areas is essential for implementing targeted mitigation measures (Yesuph, Dagnew, 2019). Nghe An Province, Vietnam, experiences a tropical monsoon climate, with annual precipitation ranging from 1,800 to 2,200 mm, and diverse topographical features (elevations from 10 m to 1,500 m). The interplay between land use, agricultural activities, and precipitation variability heightens erosion risks (Committee T.C.D.P.s, 2021). Soil erosion diminishes humus horizon thickness, agricultural output, and economic resilience, thereby exacerbating poverty and environmental degradation (Dung et al., 2020). Increased precipitation intensity further accelerates topsoil depletion and quality decline, while future land degradation is expected to escalate due to climate change and suboptimal land management practices. Implementing sustainable agricultural and forestry models is imperative to enhance socio-economic resilience and mitigate erosion. This study, conducted in Thanh Chuong District, Nghe An Province, Vietnam, evaluates the current soil erosion dynamics in a tropical monsoon environment.

2. Materials and methods

2.1. Meteorological and Geographical Conditions of the Study Area

The study area, Thanh Chuong District in Nghe An Province, spans approximately 1,228 km² and is located 45 km west of Vinh City (18°34'42"–18°53'33" N, 104°56'07"–105°36'06" E). It borders Anh Son and Do Luong districts (north), Huong Son district, Ha Tinh Province (south), Do Luong and Nam Dan districts (east), and Bolikhamxai Province, Laos (west).

The region experiences a tropical monsoon climate with distinct seasons: a hot, humid, and rainy summer (May–October) and a cooler, drier winter (November–April). Annual rainfall ranges from 1,800 to 2,200 mm, concentrated (85 %) between August and October. Relative humidity varies from 84 % to 86 %, with seasonal differences of 17–20 %. Annual evaporation is 700–940 mm. The average temperature is 23.5°C–24.5°C, peaking at 35°C–36°C in June–July and dropping to 13°C–14°C in December–February. Sunshine duration ranges from 1,500 to 1,700 hours per year. The district is influenced by the northeast monsoon (winter) and the southwest foehn wind (summer), which exacerbates drought and heat stress, impacting agriculture.

Geologically, the district comprises sedimentary, metamorphic, volcanic, and alluvial formations, with ferruginous soils dominating hilly regions and alluvial soils along river floodplains. The terrain transitions from low hills in the northeast to high mountains (900–1,026 m) in the southwest, including the Vu Tru range. The Ca River (375 km total length, 32 km within Thanh Chuong) and six other rivers provide abundant surface water. However, steep slopes, narrow river channels, and concentrated seasonal rainfall contribute to frequent floods, flash floods, and soil erosion.

2.2. Characteristics of Study Objects

To assess erosion intensity at study sites, spatio-temporal land use distribution maps were generated using Landsat (https://glovis.usgs.gov) and Sentinel (https://scihub.copernicus.eu) satellite imagery. High-resolution (30 m) image datasets spanning 2000–2021 were utilized (Appendix. Table S1).

Prior to classification, remote sensing images were preprocessed using ENVI software (version 4.7). To enhance accuracy and ensure comprehensive coverage of the study area, atmospheric correction was applied, aligning the vegetation spectral curve with real spectral reflectance. Additionally, image processing involved radiometric, atmospheric, geometric, and topographic corrections to improve data quality and analytical precision.

2.3. Land Use Spatio-Temporal Distribution Maps

Satellite Imagery. To achieve the objectives of this study, land use spatio-temporal distribution maps were generated using Landsat (https://glovis.usgs.gov) and Sentinel (https://scihub.copernicus.eu) satellite imagery. The datasets, with a spatial resolution of 30 m, were acquired for the period 2000–2021. Prior to classification, the images were processed using ENVI software (version 4.7). Atmospheric correction was applied to ensure the vegetation spectrum curve closely matched real vegetation spectra. Additional pre-processing steps included radiometric, atmospheric, geometric, and topographic corrections to enhance image accuracy.

GIS Data Utilization. The digital elevation model (DEM) dataset was selected using the grid referencing method to ensure spatial consistency across all resampled images. To enhance image quality, satellite data underwent atmospheric correction, and resolution was resampled from 30 m to 10 m. GIS-managed digital datasets were obtained from the Department of Natural Resources and Environment, including administrative maps, current land use maps, and soil maps.

Additional data sources included. Reports from the Department of Natural Resources and Environment of Nghe An Province, the Department of Agriculture and Rural Development of Nghe An Province, and the People's Committee of Thanh Chuong District. Statistical Yearbooks of Nghe An Province and Thanh Chuong District**.**

2.4. Field Survey Method

Field surveys were conducted to validate data on vegetation cover, cultivation practices, and soil erosion factors. Soil erosion severity was assessed across six land cover types: (1) natural forest restoration, (2) forest vegetation, (3) perennial vegetation, (4) annual vegetation, (5) shrub vegetation, and (6) bare land.

Cropping practices were categorized into: (1) contour cultivation of tea and citrus on hilly terrain, (2) intercropping annual crops on slopes, and (3) monoculture of acacia and cassava.

Erosion severity was classified into five levels: very low (0–5 T ha^{-1} yr^{-1}), low (5–10T ha^{-1} yr^{-1}), moderate (10–20 T ha^{-1} yr^{-1}), high (20–50 T ha^{-1} yr^{-1}), and very high (>50 T ha^{-1} yr^{-1}). Survey points were systematically distributed across Thanh Chuong District, Nghe An Province, Vietnam, ensuring representativeness

2.5. Remote Sensing Method

Pre-processing of satellite images involved stitching, straightening, filtering, and enhancement. Land cover classification was performed using the maximum likelihood classification algorithm, with accuracy assessed through ground truth validation. Field verification included marking virgin and plantation forests, perennial and annual crops, other vegetation, and water bodies using GPS-referenced field data.

Classification accuracy for Landsat images was 93 % and 88 %, while Sentinel images achieved 84 %. Land cover change (LCC) maps for 2010, 2015, and 2021, developed using the RUSLE model, were validated against ground truth data. The model demonstrated high reliability, with overall accuracy exceeding 90 %, confirming its effectiveness in simulating soil loss in the study area.

2.6. Soil Erosion Estimation Using an Optimized RUSLE Model

This study refines the Revised Universal Soil Loss Equation (RUSLE) to enhance soil erosion assessment accuracy. The RUSLE model, an advancement of the Universal Soil Loss Equation (USLE) (Wischmeier, Smith, 1978) predicts average annual soil loss through the integration of five key factors: rainfall aggressiveness (R), soil erodibility (K), slope length and steepness (LS), land cover (C), and erosion control practices (P). The optimized RUSLE model facilitates data acquisition by converting Digital Elevation Model (DEM) data into satellite imagery, improving precision compared to traditional erosion models. Our optimized RUSLE model determines the average annual soil loss using the following formula (1): $\mathbf{A=R\times K\times LS\times C\times P}$

The R-factor, representing precipitation-induced soil erosion, is computed using the equation: $\mathbf{R=79+0{,}363\times X_a}$

where X_a is the average annual precipitation (mm), derived from data collected at six observation stations (2010–2021). The Kriging interpolation method, integrated with ArcGIS, converts precipitation data into raster layers.

The K-factor quantifies soil loss potential and is determined using soil texture, organic matter content, and permeability, computed as:

$$\mathbf{K = 27.66 \times 10^{1.14} \times 10^{-8} \times (12 - a) + 0.0043 \times (b - 2) + 0.0033 \times (c - 3)}$$

where a is organic matter (%), b is soil texture, and c is soil permeability.

The LS-factor, indicating topographic influence, is calculated by:

$$\mathbf{LS} = \left[\frac{\mathbf{Q_a M}}{\mathbf{22.13}}\right]^{\mathbf{y}} \times \left(\mathbf{0.065} + \mathbf{0.045} \times \mathbf{S_g} + \mathbf{0.0065} \times \mathbf{S_g^2}\right)$$

where Qa is flow accumulation, M is grid size, Sg is slope (%), and y is an exponent (0.2–0.5). The C-factor accounts for vegetation cover, obtained from LUMP-based lookup tables. The P-factor, which represents conservation practices, is computed as:

$$\mathbf{P} = \mathbf{0.2} + \mathbf{0.03} \times \mathbf{S}$$

where S is slope (%), using the Wener approach. This optimized RUSLE model enables precise soil loss estimation by integrating high-resolution meteorological, topographical, and land use data. Its applicability enhances erosion assessment and supports sustainable land management strategies.

3. Results and discussion

3.1. Results of Soil Erosion Monitoring Using Satellite Imagery

The study utilized three satellite image sources: Landsat 5 TM, Landsat 8 OLI, and Sentinel 2A, providing comprehensive information on the study area. The diagram below (Figure 1) outlines the research stages and data processing step.

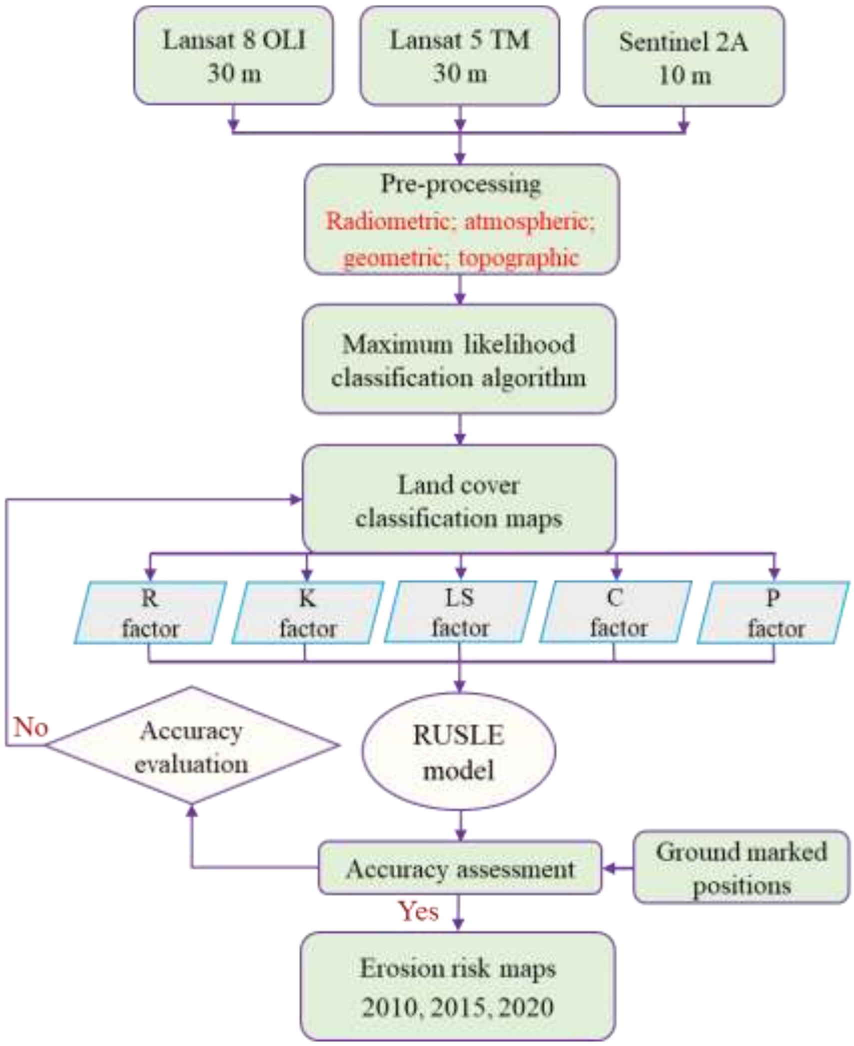

Fig. 1. Image processing workflow for erosion risk map generation

3.2. Influence of Rainfall on Soil Erosion (R-Factor)

Tropical cyclones and orographic effects significantly influence rainfall patterns in the Central Region. The Thanh Chuong study area experiences two distinct seasons: a dry season (December–April) and a rainy season (May–November). The dry season accounts for approximately 12 % of the annual rainfall, with January and February being the driest months

(33.64 mm and 24.33 mm, respectively, for 2010–2021) (Table 1).

The rainy season, contributing about 88 % of the annual precipitation, peaks from August to October, with average rainfall values of 269.46 mm (August), 468 mm (September), and 402.25 mm (October). Rainfall is primarily driven by tropical storms, often coinciding with the hurricane and flood seasons.

Table 1. Frequency of Heavy Rainfall Events and Maximum Daily Rainfall in the Study Area (2010–2021)

Year	Jan.	Feb.	Mar.	Apr.	May.	Jun.	July.	Aug.	Sep.	Oct.	Nov.	Dec.	Total Rainfall	Time
2010	0	0	0	0	0	1	0	7	0	5	0	0	211.3	25/8
2011	0	0	0	0	1	2	3	0	4	1	0	0	130.4	10/9
2012	0	0	0	0	3	0	0	2	2	0	2	0	365.9	6/9
2013	0	0	0	0	0	1	1	1	4	1	0	0	321.8	23/6
2014	0	0	0	0	0	1	0	1	1	0	0	0	152.5	13/6
2015	0	0	1	0	1	2	0	1	2	0	0	0	132.0	17/9
2016	0	0	0	0	0	0	0	0	0	1	1	0	254.1	15/10
2017	0	0	1	0	3	1	4	2	1	3	0	0	161.9	10/10
2018	0	0	0	0	0	0	4	0	2	0	1	2	188.5	19/7
2019	0	0	0	0	1	0	1	3	1	1	0	0	89.3	3/9
2020	0	0	0	0	0	0	0	2	3	4	0	0	508.6	30/10
2021	0	0	0	2	0	1	2	0	4	3	0	0	128.8	24/9
Total	**0**	**0**	**2**	**2**	**9**	**9**	**15**	**19**	**24**	**19**	**4**	**2**		

Notes: Data source is from the hydrometeorological station in the study area.

Unlike Northern Vietnam, where the rainy season begins in May under the influence of the southwest monsoon, Thanh Chuong experiences a delayed onset due to the foehn effect of southwest winds from May to August. With an annual precipitation range of 1,800–2,200 mm, the region is highly susceptible to soil erosion, particularly in mountainous areas. Although the frequency of extreme rainfall events (51–100 mm/day) is relatively low, the total precipitation is significant. Table 1 provides a summary of heavy rainfall occurrences (>50 mm/day) and maximum daily precipitation recorded between 2010 and 2021.

The highest concentration of rainfall events (Table 2) occurs from May to November, with peak daily precipitation in August, September, and October. Rainfall dynamics in the study area deviate from typical storm-induced precipitation patterns observed in other regions of Vietnam. The variability in heavy daily rainfall is significant, ranging from 89.3 mm (September 3, 2019) to 508.6 mm (October 30, 2020), the latter causing widespread flooding and high soil erosion risk.

Table 2. Annual Precipitation in the Study Area (2010–2021) (mm)

Year	Jan.	Feb.	Mar.	Apr.	May.	Jun.	July.	Aug.	Sep.	Oct.	Nov.	Dec.	Total Rainfall
2010	57.20	12.00	13.10	86.00	80.20	100.50	140.00	743.40	82.60	683.60	28.30	14.70	2,041.60
2011	41.60	11.70	77.90	21.90	126.40	291.90	384.30	172.00	538.50	272.10	76.50	46.40	2,061.20
2012	21.40	27.10	44.70	18.10	398.60	66.20	60.80	293.00	613.60	78.80	185.10	43.60	1,851.00
2013	23.30	16.50	22.00	39.30	104.00	349.20	254.50	224.90	646.50	471.70	66.30	32.40	2,250.60
2014	25.30	31.50	28.90	39.10	88.70	285.80	156.90	356.00	519.40	206.40	66.00	21.90	1,825.90
2015	30.80	27.80	154.90	78.10	78.40	163.60	160.00	266.20	560.90	190.90	125.70	49.40	1,886.70
2016	86.50	17.60	25.30	92.00	61.40	11.20	125.20	178.50	624.70	371.50	206.40	41.70	1,842.00
2017	49.70	10.70	96.30	20.20	345.80	106.50	456.70	298.20	338.40	437.40	37.10	40.20	2,237.20
2018	8.20	52.00	34.90	56.60	79.10	45.30	701.00	157.60	231.40	15.10	170.80	253.90	1,805.90
2019	20.60	19.90	29.50	51.20	81.40	1.00	134.60	186.10	587.70	577.80	139.10	42.10	1,871.00

Year	Jan.	Feb.	Mar.	Apr.	May.	Jun.	July.	Aug.	Sep.	Oct.	Nov.	Dec.	Total Rainfall
2020	31.10	23.60	82.40	83.40	102.00	17.30	65.30	288.60	259.30	1,108.90	67.80	18.30	2,148.00
2021	8.00	41.60	56.10	315.60	28.70	188.30	301.20	69.00	613.00	412.80	64.50	24.70	2,123.50

Notes: Data source is from the hydrometeorological station in the study area (2010-2021)

Besides the primary rainy season (August–October), a secondary peak occurs in May–June due to the Tropical Convergence Zone. The annual rainfall-runoff erosion coefficient (R-factor) quantifies rainfall intensity's impact on erosion and requires detailed precipitation data for accurate assessment (Wischmeier, Smith, 1978). The R-factor in the study area varies between 0.69 and 0.87 MJ mm ha^{-1} h^{-1}, with higher values recorded in southern communes (Thanh Lam, Thanh Xuan, Thanh Mai, Thanh Tung, Thanh Yen, Thanh Ha, Thanh Giang) and lower values in northern communes (Cat Van, Thanh Nho, Thanh Duc, Thanh Hoa). The R-factor is classified into six ranges: 0.69–0.72, 0.72–0.75, 0.75–0.78, 0.78–0.81, 0.81–0.84, and 0.84–0.87 MJ mm ha^{-1} h^{-1}.

Average annual precipitation data from the local hydrometeorological station were utilized to calculate the rainfall erosivity (R-factor) (Figure 2). These data serve as a basis for assessing the impact of precipitation on soil erosion dynamics in the study area.

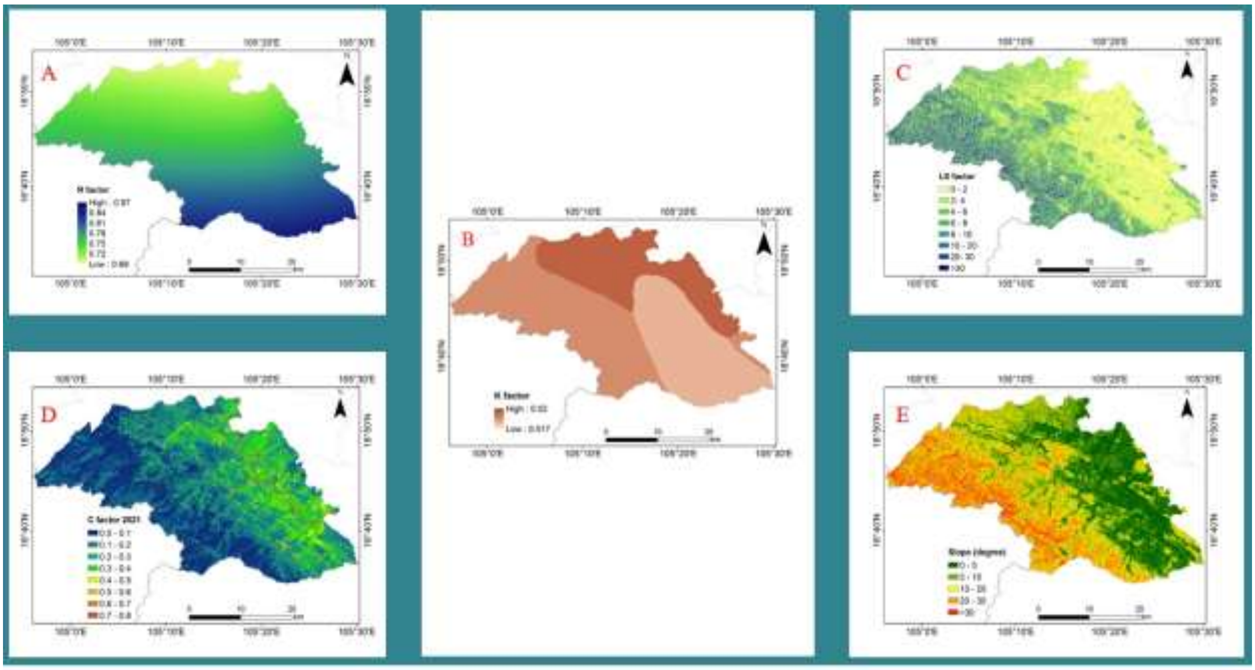

Fig. 2. Spatial Distribution of Erosion Factors in the Study Area

(A) R-Factor: Rainfall erosivity factor indicating the impact of precipitation on soil erosion; (B) K-Factor: Soil erodibility factor representing the susceptibility of soil particles to detachment and transport; (C) LS-Factor: Combined effect of slope length and steepness on erosion potential; (D) C-Factor: Land cover and management factor reflecting the influence of vegetation on soil protection; (E) P-Factor: Erosion control practices factor assessing the effectiveness of conservation measures.

3.3. Effect of Soil Type on Erosion in the Study Area (K)

The soil types in Thanh Chuong District, as identified in the Land Use Planning Report to 2030, significantly influence erosion processes.

Alluvial Soil (P). Formed by the annual deposition from the Lam and Giang River systems, alluvial soils cover approximately 17,780 hectares along both riverbanks. Their texture ranges from sandy loam to medium loam, with a pH_{KCl} value of 6.7–7.2, indicating neutral to slightly acidic conditions. These soils contain 0.25% total nitrogen, adequate phosphorus, and available potassium.

Alluvial soils on river terraces, prevalent in Thanh Van, Xuan Tuong, Thanh Duong, and Thanh Luong communes, exhibit a pH_{KCl} range of 5.8–6.8 and a texture varying from loamy to clayey. They consist of 25–50 % sand, 30–50 % humus, and 10–30 % clay, with relatively low nutrient content (total nitrogen 0.08–0.13 %, total phosphorus 0.06–0.07 %, total potassium

0.15–0.25 %). These soils typically support single-season rice cultivation, while areas with irrigation infrastructure enable double-cropping.

At higher elevations, alluvial soils are modified by agricultural activities, altering their properties. In communes such as Xuan Tuong, Thanh Van, and Vo Liet, soils exhibit greater acidity (pH_{KCl} < 5.0) and a texture ranging from medium to light loam. These soils contain minimal humus and lower concentrations of nitrogen and phosphorus (total nitrogen ~0.1%, total phosphorus 0.04–0.05 %). The presence of conglomerates in some areas further affects their erosion susceptibility.

Ferralitic Soil in the Transition Zone (Fl). Ferralitic soil (Fl) covers approximately 7,700 ha in the transition zone between hills and plains or mountains and valleys. It is characterized by strong degradation, particularly at depths of 12–25 cm, with a texture ranging from sandy loam to medium loam. The soil is highly acidic (pH_{KCl} <5.0) and has low nutrient content (N: 0.05–0.08 %, P: 0.006–0.010 %, K: 0.10–0.26 %).

In terraced fields at the base of hills, prolonged rice cultivation has altered the upper soil layer. Weathering and rainwater transport contribute to soil deposition in valley transition zones. This soil type is prevalent in Thanh Xuan, Thanh Khe, Thanh Thuy, Thanh Lam, Xuan Tuong, and Ngoc Son, with localized variations in texture and organic matter decomposition.

Yellow-Red Ferralitic Soil (Fs). This soil type originates from the weathering of shale parent rocks, exhibiting a yellow-red or red-yellow coloration. It spans approximately 29,900 hectares, predominantly distributed across various communes in the region. Thegranulometric composition varies, ranging from sandy loam to heavy silt and clay. The soil is acidic, with values pH_{KCl} ranging from 4.2 to 4.3. Organic matter content is low, varying from 1.65 % to 3.51 %, and total nitrogen ranges from 1.06% to 0.19%. Total phosphorus concentrations in the surface layer are low to moderate, while total potassium content in the upper horizon ranges from 0.93 % to 1.19 %, with a higher concentration in the deeper layers. Easily available potassium fluctuates between 7.3 and 11.2 mg/100 g of soil. The soil also contains small amounts of calcium and magnesium, and elevated concentrations of Fe_3^+ and Al_3^+.

Red-Yellow Ferralitic Soil (Fq). Formed from the weathering of sandstone, quartzite, and conglomerate, this soil type covers about 2,000 hectares, primarily in the Han Lam commune and some adjacent areas. It has a sandy loam texture with a high proportion of large sand fractions. Both its chemical and physical properties are characterized by low values.

Eroded-to-Stone Ferralitic Soil (E). This soil is derived from the weathering of various parent rocks, including shale, chalk, and quartzite, and covers an area of approximately 12,000 hectares. Historically, these areas featured thick, heavily weathered soils and dense forests with large trees. However, due to unsustainable land use practices such as indiscriminate exploitation and poor agricultural methods, significant erosion has occurred, resulting in a considerable reduction in topsoil thickness.

Yellow Mountain Ferralite Soil (H). Yellow Mountain Ferralite soil is prevalent in the mountainous regions of the study area, covering approximately 47,250 hectares, primarily between 200 to 800 meters above sea level in the western mountainous zones. The granulometric composition of this soil varies from light to medium loam. It is nitrogen-rich, with concentrations ranging from 0.1 % to 0.2 %, but is poor in phosphorus, with values ranging from 0.03 % to 0.04 %. Potassium content fluctuates between 0.2 % and 1.5 %, and the soil exhibits high acidity, with values pH_{KCl} less than 5.0. This soil type is typically covered by natural forests, though past exploitation has led to the presence of shrubbery or even bare hills in some areas. It is primarily utilized for forestry purposes.

At altitudes between 800 to 2,000 meters, the soil remains acidic, characterized by a slow rate of organic matter decomposition and a high humus content. These areas are also predominantly covered by natural forests and are mainly designated for forestry.

Soil Erosion Potential (K-Factor). The K-Factor is a critical measure of soil erosion potential, influenced by soil texture, structure, organic matter content, and water permeability (Abdo, Salloum, 2017). In the study area, the K-Factor varies as follows:

Low K-Factor (0.017 to 0.018 Mg h MJ^{-1} mm^{-1}): This range is common in the southern communes, including Thanh Lam, Thanh Xuan, Thanh Giang, Thanh Tung, Thanh Long, Vo Liet, Thanh Khe, Dong Van, and Thanh Chuong.

Medium to High K-Factor (0.018 to 0.019 Mg h MJ^{-1} mm^{-1}): Found in communes such as Thanh Thuy, Ngoc Lam, Thanh Son, Hanh Lam, and Thanh Duc.

High K-Factor (0.019 to 0.02 Mg h MJ^{-1} mm^{-1}): The highest values are observed in the northern communes, including Cat Van, Phong Thinh, Thanh Hoa, Thanh Nho, Thanh Phong, Thanh Hung, and Thanh Van. Higher K-Factor values correspond to a higher potential for soil erosion. These findings underline the importance of soil management in relation to erosion risks, particularly in areas with higher K-Factor values.

3.4. Effect of Terrain on Soil Erosion in Thanh Chuong District (LS Factor)

The terrain of Thanh Chuong District is categorized into three primary types: Plains (26 % of the total area) are primarily located along the Lam River, with small, scattered distributions. Approximately 12 % of this land experiences annual flooding. Alluvial plains support agricultural activities, including rice, corn, potatoes, and short-term industrial crops.

Hills (30 % of the area) are characterized by undulating or bowl-shaped topography, with elevations typically below 100 m. These soils, primarily formed on shale, are suitable for perennial industrial crops, fruit trees, and livestock grazing. However, unsustainable land use has resulted in soil degradation, reducing fertility and exposing rocky surfaces.

Mountains (44 % of the area) are primarily located along the Vietnam-Laos border and feature steep slopes with significant elevation variations. High mountains (>800 m) constitute 17 % of the total area, while low mountains (200–800 m) make up the remainder. The complex topography exacerbates soil erosion risk.

The LS factor, representing the impact of slope length and steepness on erosion, was analyzed using slope accumulation data. The lowest LS values were recorded in the eastern Lam River Valley (e.g., Thanh Giang, Thanh Yen, Thanh Tung), whereas the highest LS values were associated with steep, folded terrain in the southwest (e.g., Thanh Ha, Thanh Thuy, Ngoc Lam). LS values in the study area are classified into eight categories, ranging from 0 to >30, indicating increasing erosion susceptibility. Areas with steep slopes and high LS values require targeted soil conservation measures to mitigate erosion risks.

3.5. Effect of Vegetation Cover on Soil Erosion in Thanh Chuong District (C)

A comparative analysis of land cover data for 2010, 2015, and 2021 revealed significant changes in vegetation distribution across the study area (Table 3; Figure 3). Six land cover classes were identified: primary forests, forest plantations, annual plantations, perennial plantations, other land types, and water bodies.

Table 3. The land cover change during the period from 2010–2021

Cover types	Total cover area (ha)			Changed trends in periods (%)		
	2010	2015	2021	2010-2015	2015-2021	2010–2021
Primary forest	37200.2	35117.4	32797.0	-1.86	-2.07	-3.92
Plantation forest	23223.8	20233.3	20027.3	-2.67	-0.18	-2.85
Perennial plant	5659.9	4006.2	8667.6	-1.47	+4.16	+2.68
Annual plants	12002.5	17881.2	17702.9	+5.24	-0.16	+5.08
Other land	32832.0	33554.5	30951.5	+0.64	-2.32	-1.67
Water	1247.5	1377.9	2012.1	+0.12	+0.57	+0.68

In 2010, primary forests occupied the largest area (37,200.2 ha), followed by other land types (32,832.0 ha) and forest plantations (23,223.8 ha). Annual and perennial plantations covered 12,002.5 ha and 5,659.9 ha, respectively, while water bodies accounted for 1,247.5 ha. By 2015, the area of primary forests had decreased by 2,082.8 ha, shelterbelts by 2,990.5 ha, and perennial plantations by 1,653.7 ha. Concurrently, agricultural expansion led to an increase in annual plantations (+5,878.2 ha), other land types (+722.5 ha), and water bodies (+130.4 ha). This shift was primarily driven by the conversion of forested areas into agricultural land, notably for acacia and cassava cultivation (Dinh, Shima, 2022).

Between 2015 and 2021, deforestation accelerated, with forested areas shrinking by an additional 7,599.7 ha. Other vegetation types declined by 1,880.5 ha, while annual and perennial plantations expanded by 8,708.1 ha. A slight increase in water bodies (+764.6 ha) was also observed, likely resulting from the loss of forested land.

The continued decline in primary forests and shelterbelts from 2010 to 2021 underscores the intensification of land conversion for agriculture. This transformation has heightened soil erosion risks and disrupted ecological stability, emphasizing the urgent need for sustainable land management practices to mitigate degradation.

The C-Factor, representing vegetation cover and land management, is a critical parameter influencing soil erosion (El Jazouli et al., 2017). It varies according to land use and management practices (LUMP) and is referenced in established datasets (Ganasri, Ramesh, 2016). The initial C-Factor values used in this study are presented in Appendix. Table S2.

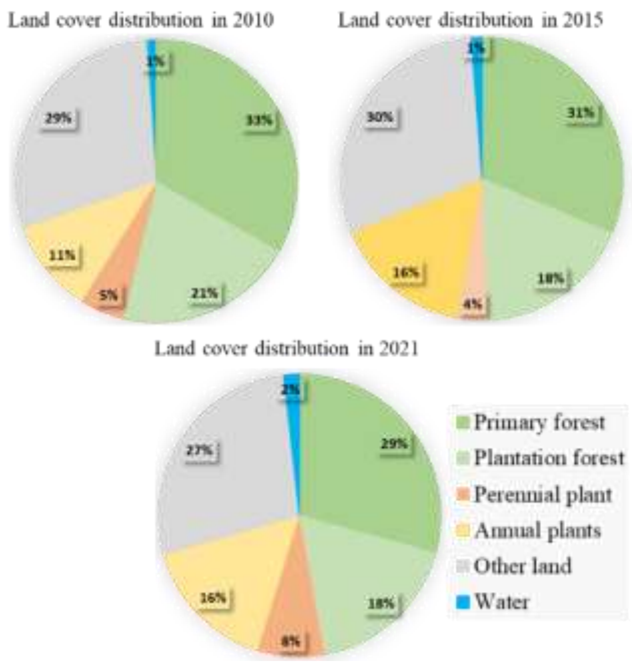

Fig. 3. Land cover distribution in the study area 2010, 2015, and 2021

To categorize the impact of vegetation on erosion, we classified the C-Factor into five ranges: 0 for water bodies, 0–0.1 for primary forests and shelterbelts, 0.1–0.3 for perennial plantations, 0.3–0.5 for annual plantations, and 0.5–0.8 for other land types (Figure 2D). Our findings indicate that a significant portion of the study area is covered by natural forests and shelterbelts, where the C-Factor is low, suggesting reduced susceptibility to soil erosion. Conversely, areas dominated by annual crops and bare soil exhibit higher C-Factor values, indicating increased erosion potential. These results highlight the protective role of forested areas in mitigating soil degradation.

3.6. Impact of Conservation Measures on Soil Erosion (P-Factor)

The P-Factor quantifies soil loss due to anthropogenic influences and is determined based on erosion control measures implemented on slopes. It represents a soil loss coefficient, which is assigned according to specific land management practices (Figure 2E).

Areas with effective soil conservation techniques typically exhibit lower P-Factor values, as these practices reduce runoff velocity and promote sediment deposition on slopes. Soil erosion potential, driven by runoff from precipitation, is influenced by both land management and basin characteristics.

Our analysis indicates that the P-Factor is primarily controlled by slope gradient, which is categorized into five classes: 0–5, 5–10, 10–20, 20–30, and >30. The study area exhibits a clear spatial differentiation in slope distribution, with the highest values observed in the western and southern regions, while a gradual decrease is noted toward the east and southeast (Figure 2E). These findings emphasize the need for targeted conservation strategies in areas with steeper slopes to mitigate soil erosion risks.

3.7. Soil Erosion Map of the Study Area

The soil erosion risk map (Figure 4A) illustrates the spatial distribution of soil loss across the study area, with values ranging from 0 to 50 t ha^{-1} yr^{-1} for the period 2010–2021. The estimated average soil loss of 25 t ha^{-1} yr^{-1}, based on RUSLE model indicators, aligns with field observations.

The analysis reveals that high soil erosion is primarily concentrated in areas with steep slopes and high precipitation intensity, particularly in the southwestern and northeastern regions. In contrast, low erosion levels are predominant across most of the study area, corresponding to regions with stable vegetation cover and gentler slopes. Approximately 18 % of the total area falls within the high to very high erosion risk categories, with moderate soil erosion occurring along a northwest-to-southwest corridor where steep slopes coincide with unsustainable operational activities (UOA).

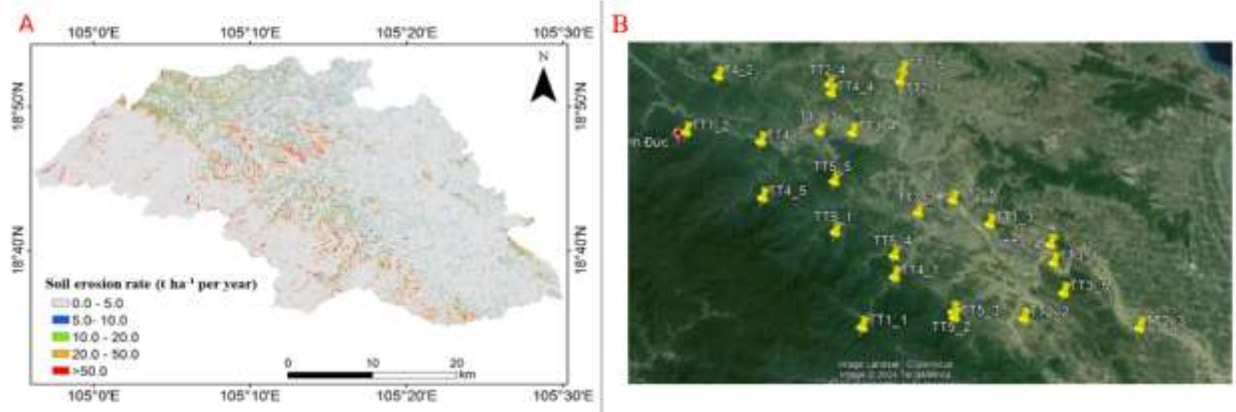

Fig. 4. (A) Soil erosion map of the study area and (B) erosion verification points

The east, southeast, and northwest regions exhibit moderate soil erosion, attributed to lower rainfall intensity and the prevalence of less steep terrain. However, land cover changes particularly the conversion of primary and plantation forests into agricultural and barren lands have contributed to increased soil loss. This is consistent with findings by Brodie & Catherine (2020), which highlight the protective role of forest and plantation vegetation in mitigating soil erosion.

Verification points (Figure 4B) were selected across the study area, focusing on representative locations within Thanh Chuong District, Nghe An Province, Vietnam. Temporal image analyses suggest that fluctuations in land cover significantly influence the C-Factor, thereby accelerating soil loss. These findings underscore the importance of sustainable land management practices to mitigate erosion risks.

3.8. Development of Erosion Control Measures in the Study Area

Impact of Human-Induced Erosion on Forest Soil Degradation. Anthropogenic soil erosion is a major contributor to forest soil degradation worldwide, directly influencing forest stand development and reducing forest productivity. Sustainable forest management requires an accurate assessment of soil loss resulting from various forestry activities. A key factor in this process is rainfall intensity, which affects the volume of rainwater reaching the soil. This is closely linked to phytosanitary conditions, as the stability and health of forest stands depend on canopy consistency and vegetation density.

Determination of Vegetation Cover Threshold and Anti-Erosion Efficiency. In central Vietnam, where 80 % of the land area is characterized by sloping terrain, soil erosion is exacerbated by both natural factors and human activities, leading to severe ecological imbalances. To quantify the erosion control efficiency of forest stands, it is crucial to evaluate parameters such as tree density, seedling biomass, and surface runoff rates. These factors influence precipitation retention capacity, thereby reducing erosion intensity. Determining the optimal number of trees per hectare, alongside the presence of shrubs, seedlings, and forest litter, is essential for minimizing soil loss. Consequently, a comprehensive strategy is required to enhance land-use management practices, particularly in erosion-prone zones at the regional level.

Development of Agricultural and Forestry Models for Heavily Eroded Lands. At the local level, effective erosion control measures remain underdeveloped due to limited methodological frameworks and insufficient technological support. One of the most promising approaches is Sloping Agriculture Land Technology (SALT), an integrated soil conservation and agroforestry system designed for erosion-prone landscapes. SALT incorporates contour farming techniques, where strips of perennial and nitrogen-fixing trees (spaced 3 to 5 meters apart) are planted between rows of food and cash crops. This system enhances soil retention, reduces runoff velocity, and improves land productivity while ensuring sustainable agricultural and forestry land use in severely eroded regions.

Implementation of the SALT 3 Model in Livestock Farming. Anthropogenic soil erosion often results from poor land management, particularly in livestock farming, where improper waste disposal and overgrazing accelerate land degradation. The SALT 3 model offers an integrated approach that combines small-scale afforestation with food production, ensuring environmental sustainability while enhancing agricultural productivity.

This model promotes an optimal land-use structure of 40 % agricultural land and 60 % forestry, effectively balancing soil conservation and economic benefits. The expansion of forest cover within agricultural systems increases the availability of food, fuelwood, and other forest-based products, directly benefiting farmers' incomes. The SALT 3 model is particularly suitable for land areas of 5-10 hectares and can be adapted to various terrain types.

Experimental application of this model indicates that diversification of perennial crops is crucial for sustainable land use. Ideally, at least 20 % of total planted trees should be perennial species, contrasting with the current trend in the study area, where acacia monoculture dominates.

Application of the SALT 1 Model in Tea Plantations. The SALT 1 model integrates annual and perennial crops in a structured manner, ensuring soil compatibility and consistent harvesting cycles. Currently, tea plantations on hills are cultivated along contour lines, but lack protective strips of nitrogen-fixing trees, which are essential for erosion control, shading, soil enrichment, and sustainable timber production.

Under this model, nitrogen-fixing trees are planted in dense double rows between tea crops. Once these trees reach 1 meter in height, their branches are pruned, and leaves are used as organic mulch, enhancing soil fertility and moisture retention. In Thanh My and Thanh Huong communes, the cropping pattern follows a 75 % agricultural – 25 % forest crop distribution, with agricultural lands divided into 50 % annual and 25 % perennial crops.

The SALT 1 model has proven economically beneficial, increasing farmers' income by 1.5 times compared to traditional cassava cultivation. Additionally, it reduces soil erosion by 50 % compared to conventional farming methods on sloping terrain. In areas where tea plantations lack forest buffers, it is essential to plant additional contour-aligned trees, prioritizing nitrogen-fixing species. These practices prevent soil erosion, enhance shade coverage, improve soil fertility, and support timber production. In Thanh Mai, Thanh An, and Thanh Thuy communes, the SALT 1 model proposes a 75 % tea plantation – 25 % forest tree structure, offering a more sustainable alternative to the existing tea cultivation systems in these hilly regions.

The SALT 4 model integrates citrus cultivation (e.g., orange and grapefruit) with food crops, focusing on perennial trees to enhance soil stability and reduce erosion. This model, effective in Thanh Nho, Thanh Duc, Thanh Lien, Thanh Thinh, and Thanh My communes, promotes soil fertility through nitrogen-fixing plants and offers economic benefits via the production of marketable fruit.

To mitigate soil erosion, trenching and embankment construction divide slopes into smaller sections, reducing runoff speed and improving water infiltration. The spacing between barriers varies with slope steepness: 3–4 meters for steep slopes and 5–6 meters for moderate ones. In areas with rocky terrain, stone barriers provide an alternative solution. In gentle slopes, the construction of terraces is an effective strategy for long-term erosion control. This involves determining terrace dimensions based on soil type, constructing embankments to slow runoff, and redistributing fertile topsoil to enhance productivity.

The SALT 4 model emphasizes the cultivation of perennial crops, such as oranges, which offer benefits including nitrogen fixation, erosion control, and soil improvement while also providing a marketable food product. In contrast, the SALT 1 model applied to tea plantations involves a combination of annual crops interspersed with perennial species to optimize soil conditions and ensure consistent harvests. The cropping structure proposed for this model includes 75 % agricultural crops and 25 % forest crops, with 50 % of agricultural crops being annuals and 25 % perennials. Overall, the SALT models provide a holistic approach to erosion control and sustainable land management, enhancing agricultural productivity while preserving soil integrity.

4. Conclusion

This study provides a comprehensive assessment of soil erosion in Thanh Chuong District, Nghe An Province, Vietnam, under tropical monsoon conditions. Utilizing GIS, remote sensing, and an optimized RUSLE model, it identifies high erosion risk areas and quantifies soil loss, averaging 25 t/ha/year, with 18 % of the region facing high to very high erosion. Key factors influencing erosion include rainfall intensity, slope, soil type, and land use practices. The findings highlight the urgent need for targeted conservation measures, such as SALT-based agroforestry models, vegetation restoration, and terracing, to promote sustainable land management and mitigate soil degradation in erosion-prone areas.

5. Conflict of interest

The authors have no conflicts of interest to declare that are relevant to the content of this article.

References

Abdo, Salloum, 2017 – *Abdo, H., Salloum, J.* (2017). Mapping the soil loss in Marqya basin: Syria using RUSLE model in GIS and RS techniques. *Environmental Earth Sciences*. 76: 1-10.

Adornado et al., 2009 – *Adornado, H.A., Yoshida, M., Apolinares, H.A.* (2009). Erosion vulnerability assessment in REINA, Quezon Province, Philippines with raster-based tool built within GIS environment. *Agricultural Information Research*. 18(1): 24-31.

Aksoy, Kavvas, 2005 – *Aksoy, H., Kavvas, M.L.* (2005). A review of hillslope and watershed scale erosion and sediment transport models. *Catena*. 64(2-3): 247-271.

Committee T.C.D.P.s, 2021 – Committee T.C.D.P.s. Report on Land Use Planning to 2030 of Thanh Chuong District, 2021.

Dinh, Shima, 2022 – *Dinh, K.H.T., Shima, K.* (2022). Effects of forest reclamation methods on soil physicochemical properties in North-Central Vietnam. *Research on Crops*. 23(1): 110-118.

Dung et al., 2020 – *Dung, N.D. et al.* (2020). Study on the characteristics of sedimentation soil of small and medium reservoirs in Ha Tinh. *Journal of Water resources & Environmental engineering*. 60: 99-106.

El Jazouli et al., 2017 – *El Jazouli, A. Barakat, A., Ghafiri, A, El Moutaki, S, Ettaqy, A. Khellouk, R.* (2017). Soil erosion modeled with USLE, GIS, and remote sensing: a case study of Ikkour watershed in Middle Atlas (Morocco). *Geoscience Letters*. 4(1): 25.

Ganasri, Ramesh, 2016 – *Ganasri, B., Ramesh, H.* (2016). Assessment of soil erosion by RUSLE model using remote sensing and GIS-A case study of Nethravathi Basin. *Geoscience Frontiers*. 7(6): 953-961.

Golkarian et al., 2023 – *Golkarian, A., Khosravi, K., Panahi, M., Clague, J.J.* (2023). Spatial variability of soil water erosion: Comparing empirical and intelligent techniques. *Geoscience Frontiers*. 14(1): 101456.

Le Dinh et al., 2022 – *Le Dinh, H., Shibata, M., Kohmoto, Y., Ho, L.N., Funakawa, S.* (2022). Analysis of the processes that generate surface runoff and soil erosion using a short-term water budget on a mountainous sloping cropland in central Vietnam. *Catena*. 211: 106032.

Tian et al., 2008 – *Tian, W. et al.* (2008). The status of soil and water loss and analysis of countermeasures in China. *Research of soil and water conservation*. 15(4): 204-209.

Wischmeier, Smith, 1978 – *Wischmeier, W.H., Smith, D.D.* (1978). Predicting rainfall erosion losses: a guide to conservation planning. *Department of Agriculture, Science and Education Administration*. P. 537.

Yesuph, Dagnew, 2019 – *Yesuph, A.Y., Dagnew, A.B.* (2019). Soil erosion mapping and severity analysis based on RUSLE model and local perception in the Beshillo Catchment of the Blue Nile Basin, Ethiopia. *Environmental Systems Research*. 8(1): 1-21.

Appendix

Table S1. Satellite imagery data utilized in this study

Data	Projection	Date of receipt	Resolution (m)	Source
Landsat 5 TM	UTM-Zone-48N	2000	30	https://glovis.usgs.gov/
Landsat 5 TM	UTM-Zone-48N	2001	30	https://glovis.usgs.gov/
Landsat 5 TM	UTM-Zone-48N	2002	30	https://glovis.usgs.gov/
Landsat 5	UTM-Zone-48N	2003	30	https://glovis.usgs.gov/

Data	Projection	Date of receipt	Resolution (m)	Source
TM				
Landsat 5 TM	UTM-Zone-48N	2004	30	https://glovis.usgs.gov/
Landsat 5 TM	UTM-Zone-48N	2005	30	https://glovis.usgs.gov/
Landsat 5 TM	UTM-Zone-48N	2006	30	https://glovis.usgs.gov/
Landsat 5 TM	UTM-Zone-48N	2007	30	https://glovis.usgs.gov/
Landsat 5 TM	UTM-Zone-48N	2008	30	https://glovis.usgs.gov/
Landsat 5 TM	UTM-Zone-48N	2009	30	https://glovis.usgs.gov/
Landsat 5 TM	UTM-Zone-48N	2010	30	https://glovis.usgs.gov/
Landsat 5 TM	UTM-Zone-48N	2011	30	https://glovis.usgs.gov/
Landsat 5 TM	UTM-Zone-48N	2012	30	https://glovis.usgs.gov/
Landsat 8 OLI	UTM-Zone-48N	2013	30	https://glovis.usgs.gov/
Landsat 8 OLI	UTM-Zone-48N	2014	30	https://glovis.usgs.gov/
Landsat 8 OLI	UTM-Zone-48N	2015	30	https://glovis.usgs.gov/
Sentinel 2A	UTM-Zone-48N	2016	10	https://scihub.copernicus.eu/
Sentinel 2A	UTM-Zone-48N	2017	10	https://scihub.copernicus.eu/
Sentinel 2A	UTM-Zone-48N	2018	10	https://scihub.copernicus.eu/
Sentinel 2A	UTM-Zone-48N	2019	10	https://scihub.copernicus.eu/
Sentinel 2A	UTM-Zone-48N	2020	10	https://scihub.copernicus.eu/
Sentinel 2A	UTM-Zone-48N	2021	10	https://scihub.copernicus.eu/

Table S2. C-Factor for Various Land Use and Management Practices in the Study Area

Class	C factor range	Mean value
Primary forest	0.001-0.002	0.0015
Plantation forest	0.01-0.02	0.015
Perennial plant	0.1-0.3	0.2
Annual plants	0.3-1.0	0.65
Other land	0.5-1.0	0.75
Waterbody	0	0